Optical-Fiber Based Fluorescence Detection System

An optical fiber based fluorescence detection system was developed to measure the concentration of FITC-BSA in the abluminal chamber in real-time. This cost-effective and compact system used a light emitting diode (LED) as excitation light source and an ultra sensitive photodiode as photon detector. The design was based on similar systems used in previous studies as described by Novak et al. (24), DeMaio et al. (9), Yang et al. (34) and in (26).

Fig. S6 is the schematic of the light path. Excitation lights from a high power blue LED (MBLED, peak wave length 470 nm, 625 mW, Thorlabs) were collimated by a plano-convex lens (f=25.4 mm, surface coated for 350-650 nm wavelength light transmission, Thorlabs). Blue excitation light was then filtered by a narrow bandpass filter (470 nm/10 nm, central wavelength/ full width at half maximum, Thorlabs), and reflected by a long pass dichroic mirror (Q505LP, Chroma) placed at 45 degree to the light path. Excitation light was finally focused by another plano-convex lens (f=25.4 mm, Thorlabs) to one end of the polymer clad multimode silica fiber (numerical aperture 0.48, 1 mm core diameter, Thorlabs). The other end, the measurement end, of the optical fiber was immersed in the abluminal solution. Both ends of the fiber were polished by 5 μm, 3 μm and 1 μm aluminum oxide polishing sheet (Thorlabs) sequentially to achieve the best transmission efficiency.

The emitted fluorescence light was collected by the same optical fiber and collimated by the same lens. The fluorescence light passed through the dichroic mirror, filtered by an emitter filter (530 nm/ 10 nm, Thorlabs) and was finally focused by another

plano-convex lens (f=25.4 mm, Thorlabs) to the sensor of an ultra-sensitive femtowatt photoreceiver (PDF10A, Thorlabs). The photoreceiver combines a low noise silicon photodiode with a built-in ultra low noise transimpedance amplifier with a high gain of 10^{12} V/A. All the optical components were enclosed in lens tubes (Thorlabs) and a mirror holder was used to secure the dichroic mirror precisely at the 45 degree position. Thus, the entire optical path, except for the measurement end of the fiber, was shielded from stray light. The controllers of the LED and photoreceiver were connected to a DAQ board (NI PCI-6221, National Instruments) through BNC cables. The LED was turned on only during the measurement time to minimize photo bleaching. The output of the LED was controlled by a rectangular voltage signal at 20 Hz generated by the DAQ. The average excitation intensity can be modulated by altering either the duty cycle or peak voltage of the control signal. The DC voltage output from the photoreceiver was also transmitted to the computer via the DAQ board. A LabView (National Instruments) program was used for the LED control and data acquisition.

To increase the detection sensitivity and minimize the noise from stray light that enters the measurement end of the fiber, a virtual lock-in amplifier was implemented in the LabView program (1). The fluorescence signal had a frequency of 20 Hz due to the frequency of the excitation lights. An internal sinusoidal waveform of 20 Hz was generated virtually in the LabView program. The virtual lock-in amplifier then acted as a narrow bandpass filter around the reference signal frequency, thus only amplifying the signal at 20 Hz. The fluorescence measurement can be performed inside a conventional cell incubator without the effect of the ambient light. During each measurement cycle,

the LED was turned on for only 6 seconds. Two seconds after the LED was switched on and when the LED output was stable, the fluorescence signal was acquired for 4 seconds. Fluorescence measurements were fully automated, and the tracer concentration can be measured every minute to obtain $\Delta C_s/\Delta t$ for the permeability calculation.

Fig. S7 shows the measurements of a series dilution of FITC-BSA solution from 100 ng/ml to 1 μg/ml using three different excitation intensities. The peak voltages of the LED control signal were set to 0.5, 1.0 and 1.5V, respectively. The detection system demonstrated a good sensitivity and the R values of the linear regressions are greater than 0.998. Although 1.5V offered the best linearity and sensitivity, the high excitation intensity can lead to greater photobleaching and fluorescence signal saturation at lower concentrations, which limits the dynamic range of the measurements. Thus, the voltage of 1.0 V was used to control the LED output in the following experiments.

Figure S1

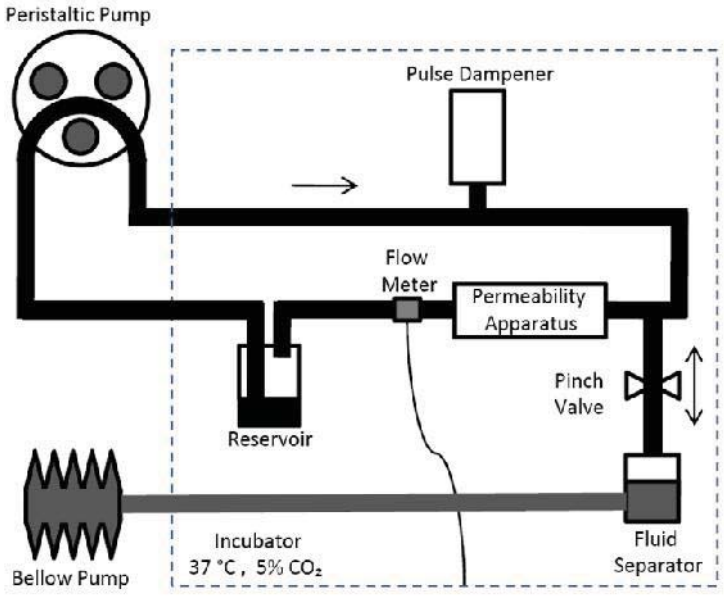

Figure S1: Schematic of the flow circuit for permeability measurement.

Figure S2

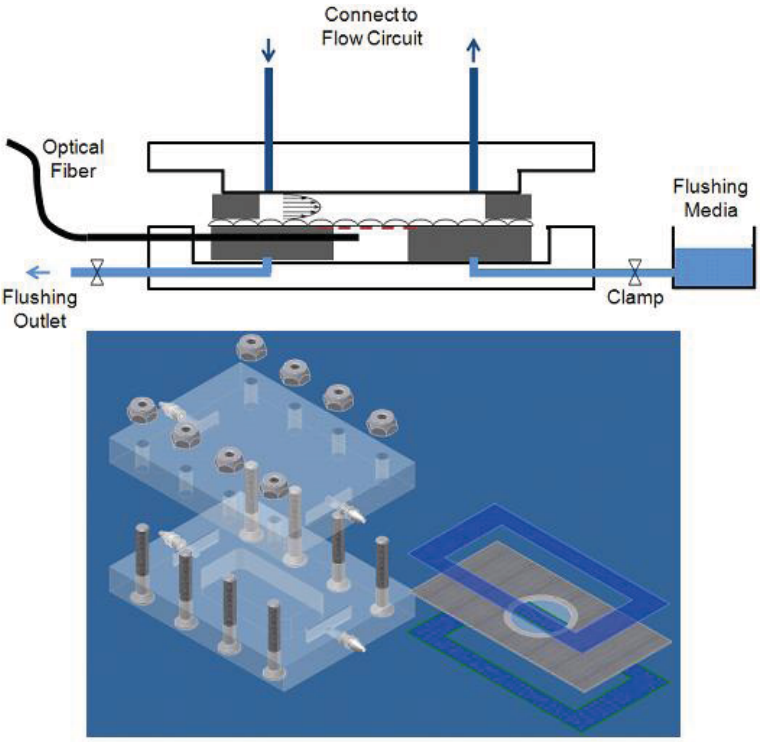

Figure S2: Schematic and 3D design of the permeability apparatus

Figure S3

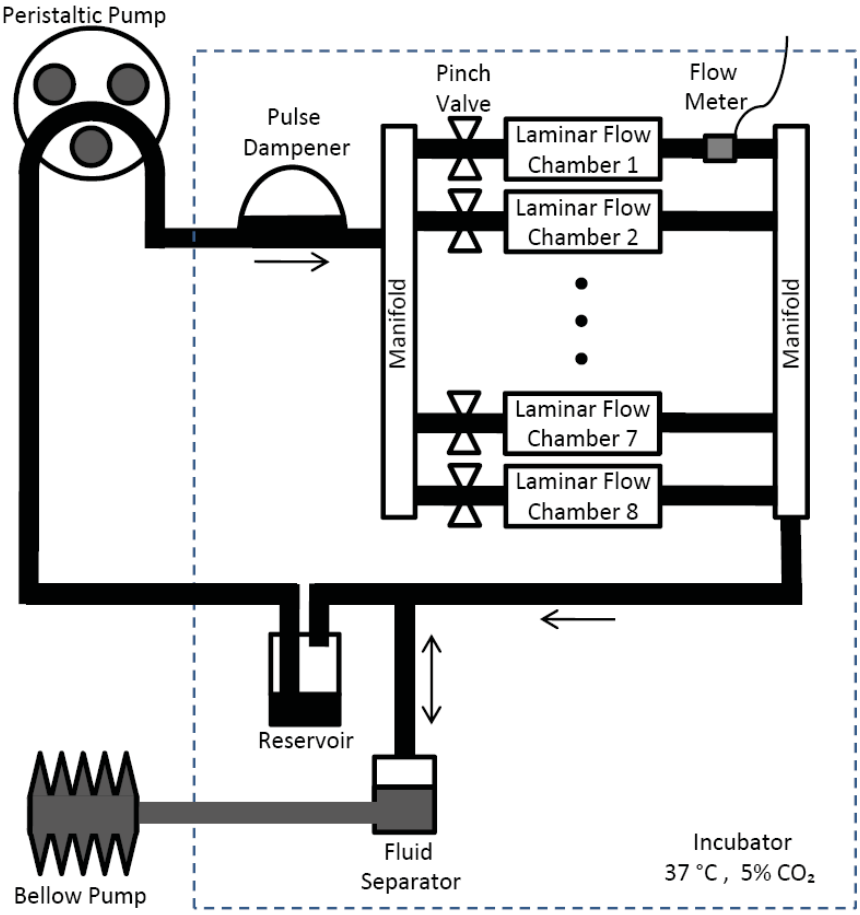

Figure S3: Schematic of flow circuit for transcriptional studies.

Figure S4

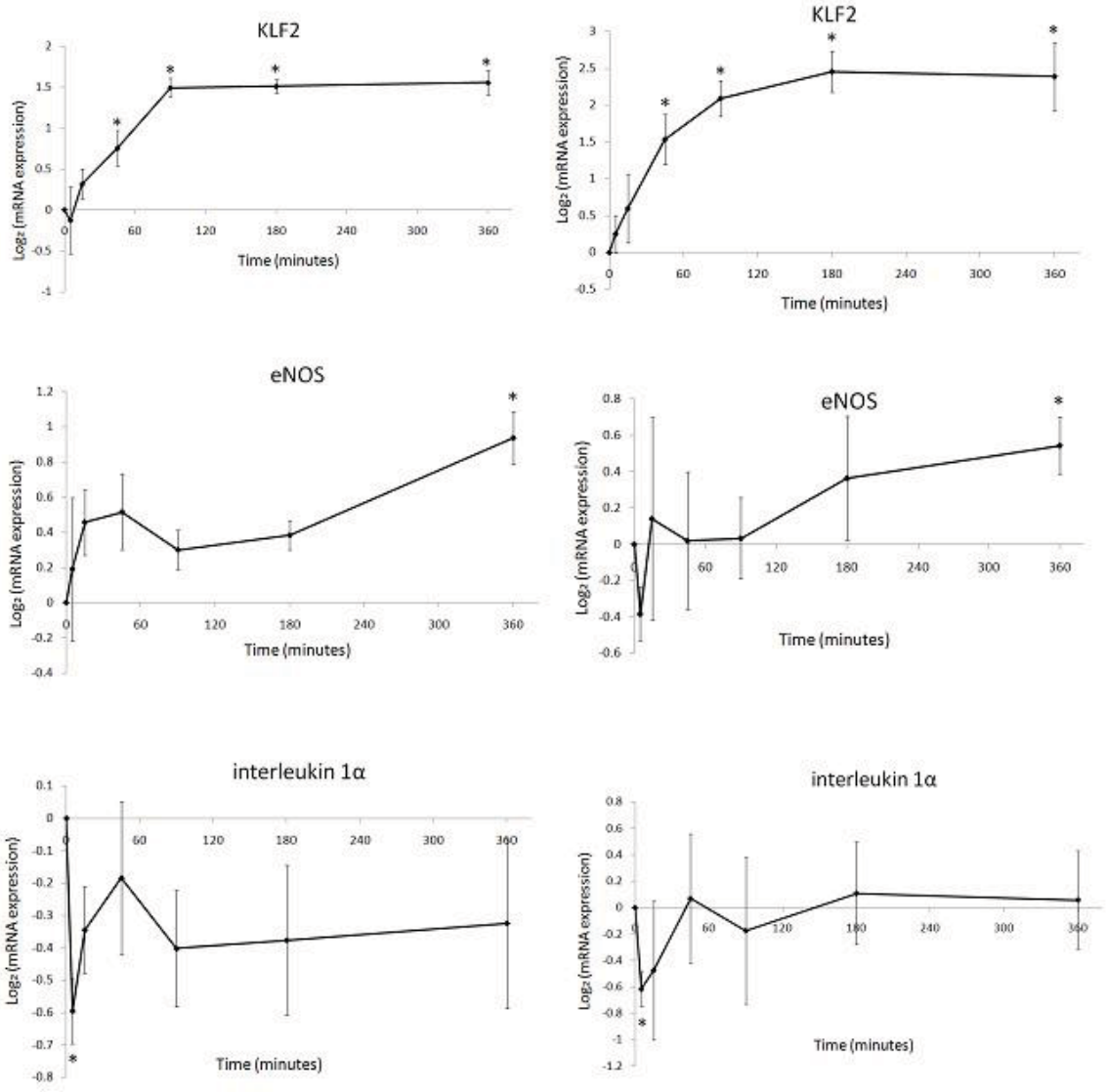

Figure S4: Real-time PCR validates the microarray results of the magnitude step-up experiments. Left: microarray measurements; Right: real-time PCR measurements. n=4 for each data point. Expression values were normalized by the pre step-up controls, and error bars indicates the standard error of the mean. *: $p<0.05$, one-way t-test against zero.

Figure S5

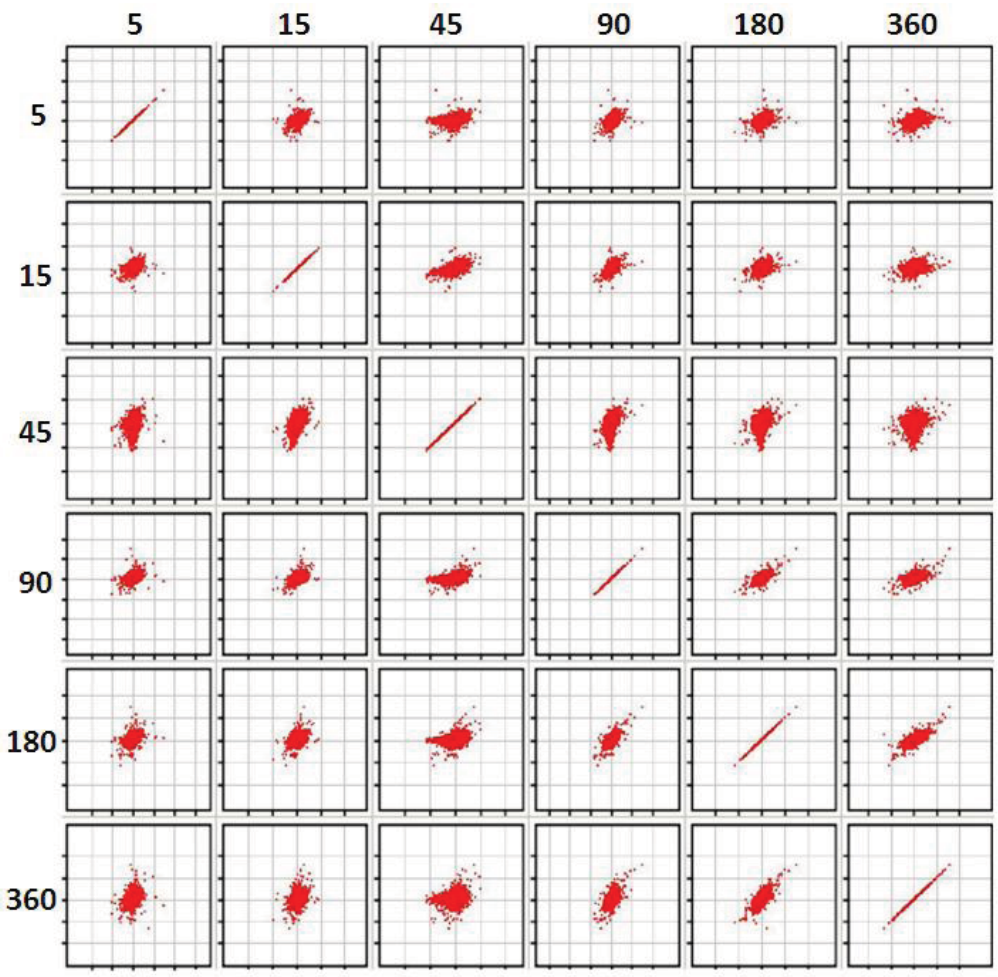

Figure S5: Matrix of scatter plots to compare the global expression profiles between different time points. Each panel compares transcriptional profile between two time points. Each gene is plotted as one data point, where x-axis is the expression value at one time point and y-axis is the expression value at the other time point.

Figure S6

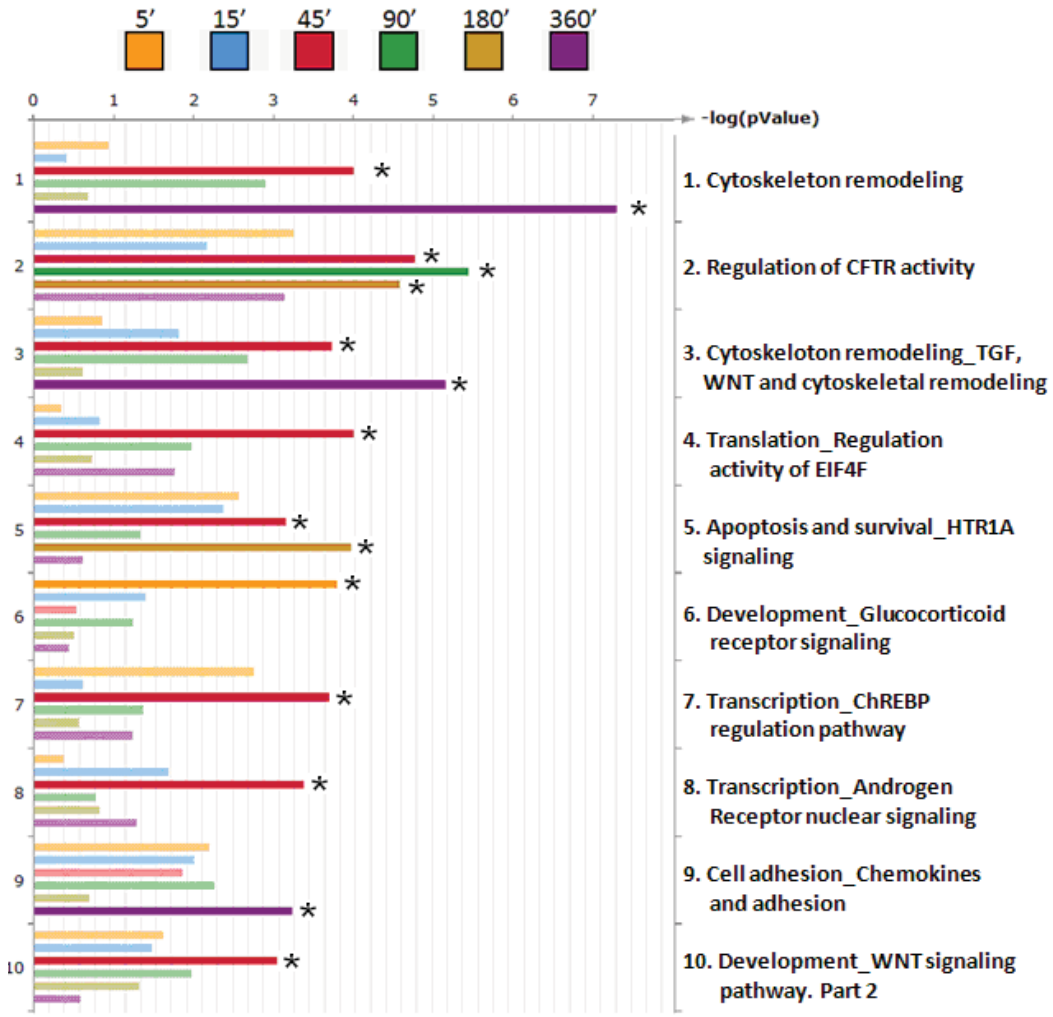

Figure S6: GeneGo identified pathways that are sensitive to the elevated shear stress magnitude. Top ten canonical pathways were listed. * indicates the false discovery rate < 5%.

Figure S7

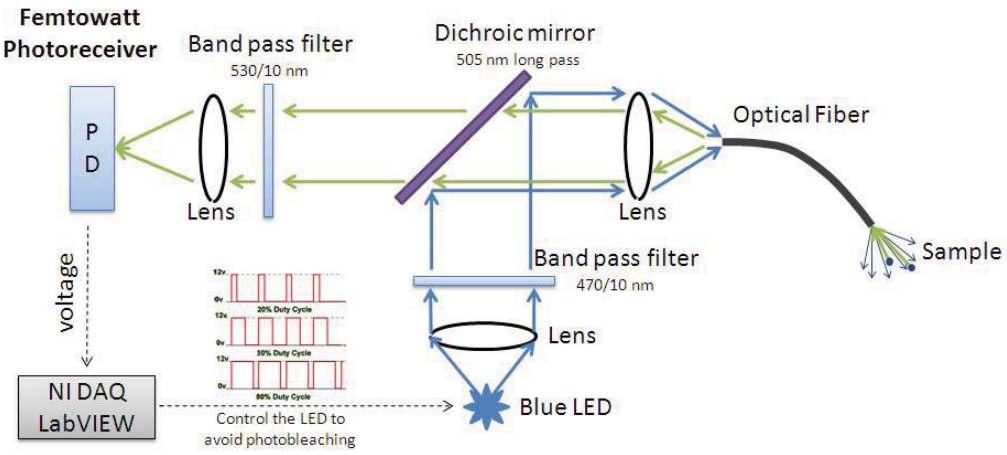

Figure S7: Schematic of the light path of the fluorescence detection system.

Figure S8

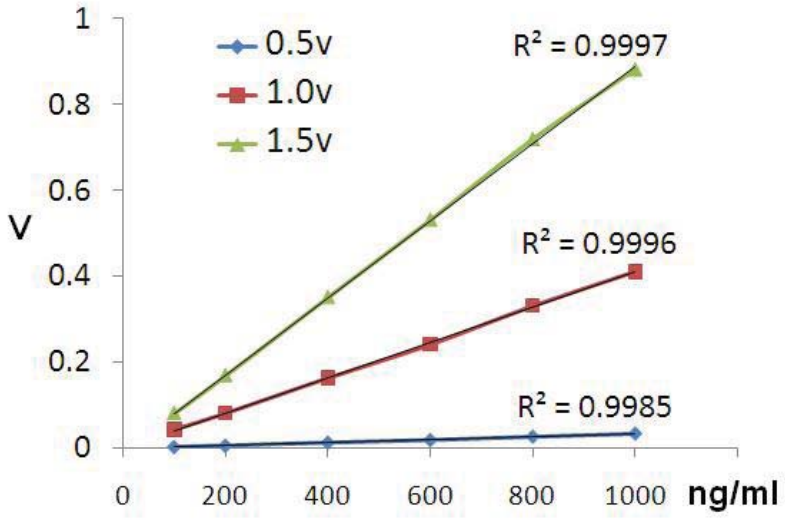

Figure S8: Measurement of a series dilution of FITC-BSA solution. X: concentrations of the FITC-BSA solution. Y: output voltages of the fluorescence detector. Excitation lights at three different intensity levels were generated by applying different driving voltage to the LED.

Table S1: Primers for real-time quantitative-PCR

Gene	3' Primer	5' Primer
GAPDH	5'–GTC TTC TGG GTG GCA GTG AT–3'	5'–GGG CAT GAA CCA TGA GAA GT–3'
eNOS	5'–AGC ACA GC AGG TTG ATT TC–3'	5'–GGC TGG TAC ATG AGC ACA GA–3'
KLF2	5'–CAA AAT GCC ACC TGT CTT CC–3'	5'–AGC CCA CCG GGT CTA CAC TA–3'
Interluekin-1α	5'–CAT CAT TCA GGA TGC ACT GG–3'	5'–CAA GGA CAG TGT GGT GAT GG–3'

Table S2: List of genes identified at different time points after shear step-up at false discovery rate controlled at 10%. The expression values were normalized to the pre step-up controls, and were presented in log2 scale.

ID	Gene	Expression	Description
5 minutes			
SS00010196	IL1A	-0.60	interleukin 1, alpha
SS00010211		-0.41	
15 minutes			
SS00003206	ZFP106	0.59	zinc finger protein 106 homolog (mouse)
SS00003440	ACTC	0.45	actin, alpha, cardiac muscle
SS00010237		0.33	
45 minutes			
SS00009868	MYH9	1.00	myosin, heavy polypeptide 9, non-muscle
SS00000396	CCAR1	0.69	cell division cycle and apoptosis regulator 1
SS00007343	LMNB1	0.53	lamin B1
SS00009180	PCDH7	0.53	BH-protocadherin (brain-heart)
SS00008997	YAF2	0.51	YY1 associated factor 2
SS00006138	C3ORF17	0.49	Chromosome 3 open reading frame 17
SS00008956		0.48	
SS00001082	SCAMP1	0.40	secretory carrier membrane protein 1
SS00004979	KIAA1279	0.37	KIAA1279
90 minutes			
SS00000203	KLF2	1.50	Kruppel-like factor 2 (lung)
SS00006925	ID1	1.13	inhibitor of DNA binding 1, dominant negative helix-loop-helix protein
SS00004771	GADD45B	0.98	growth arrest and DNA-damage-inducible, beta
SS00007520	KLF4	0.92	Kruppel-like factor 4 (gut)
SS00007619	ID2	0.79	inhibitor of DNA binding 2, dominant negative helix-loop-helix protein
SS00006583	COL4A1	0.60	collagen, type IV, alpha 1
SS00003206	ZFP106	0.60	zinc finger protein 106 homolog (mouse)
SS00009712	TIMP3	0.58	tissue inhibitor of metalloproteinase 3 (Sorsby fundus dystrophy, pseudoinflammatory)
SS00000220	ID2	0.57	inhibitor of DNA binding 2, dominant negative helix-loop-helix protein
SS00003201	LOC51136	0.54	PTD016 protein

SS00008254	BHLHB2	0.54	basic helix-loop-helix domain containing, class B, 2
SS00010237		0.44	
SS00007441	KLF10	0.43	Kruppel-like factor 10
SS00001410	ID3	0.42	inhibitor of DNA binding 3, dominant negative helix-loop-helix protein
SS00007031	SGK	0.41	serum/glucocorticoid regulated kinase
SS00000868	PTTG1	0.40	pituitary tumor-transforming 1
SS00004979	KIAA1279	0.39	KIAA1279
SS00009988	TRPC3	0.35	transient receptor potential cation channel, subfamily C, member 3
SS00001680	CD83	0.32	CD83 antigen (activated B lymphocytes, immunoglobulin superfamily)
180 minutes			
SS00000203	KLF2	1.51	Kruppel-like factor 2 (lung)
SS00007520	KLF4	1.17	Kruppel-like factor 4 (gut)
SS00006925	ID1	0.99	inhibitor of DNA binding 1, dominant negative helix-loop-helix protein
SS00007619	ID2	0.87	inhibitor of DNA binding 2, dominant negative helix-loop-helix protein
SS00009975	KCNN4	0.79	potassium intermediate/small conductance calcium-activated channel, subfamily N, member 4
SS00003184	WASL	0.75	Wiskott-Aldrich syndrome-like
SS00006914	DSIPI	0.75	delta sleep inducing peptide, immunoreactor
SS00000220	ID2	0.72	inhibitor of DNA binding 2, dominant negative helix-loop-helix protein
SS00005051	LOC401137	0.63	hypothetical LOC401137
SS00008118	STK38L	0.63	serine/threonine kinase 38 like
SS00007835	LOC401137	0.54	hypothetical LOC401137
SS00009553	TEK	0.52	TEK tyrosine kinase, endothelial (venous malformations, multiple cutaneous and mucosal)
SS00000205	FAM26B	0.50	family with sequence similarity 26, member B
SS00000537	GJA4	0.46	gap junction protein, alpha 4, 37kDa (connexin 37)
SS00000587	HMOX1	0.45	heme oxygenase (decycling) 1
SS00001680	CD83	0.39	CD83 antigen (activated B lymphocytes, immunoglobulin superfamily)
SS00007712		0.37	
SS00008566	YWHAH	0.35	tyrosine 3-monooxygenase/tryptophan 5-monooxygenase activation protein, eta polypeptide
SS00009439		0.35	
SS00006985	DOK4	0.26	docking protein 4
SS00001142	KIT	-0.33	v-kit Hardy-Zuckerman 4 feline sarcoma viral oncogene homolog
SS00003482	TTC5	-0.36	tetratricopeptide repeat domain 5
SS00007051		-0.41	
SS00004185	RGS2	-0.69	regulator of G-protein signalling 2, 24kDa
SS00001048	HLA-A	-0.69	major histocompatibility complex, class I, A
SS00005446	CXCR4	-0.77	chemokine (C-X-C motif) receptor 4
SS00002290	CXCR4	-0.81	chemokine (C-X-C motif) receptor 4
360 minutes			
SS00000203	KLF2	1.56	Kruppel-like factor 2 (lung)
SS00006925	ID1	1.36	inhibitor of DNA binding 1, dominant negative helix-loop-helix protein

SS00007520	KLF4	1.30	Kruppel-like factor 4 (gut)
SS00009782	HTR2B	1.22	5-hydroxytryptamine (serotonin) receptor 2B
SS00009975	KCNN4	1.16	potassium intermediate/small conductance calcium-activated channel, subfamily N, member 4
SS00007619	ID2	1.08	inhibitor of DNA binding 2, dominant negative helix-loop-helix protein
SS00000510	NOS3	0.94	nitric oxide synthase 3 (endothelial cell)
SS00009004	13CDNA73	0.90	hypothetical protein CG003
SS00006583	COL4A1	0.86	collagen, type IV, alpha 1
SS00000220	ID2	0.85	inhibitor of DNA binding 2, dominant negative helix-loop-helix protein
SS00000587	HMOX1	0.77	heme oxygenase (decycling) 1
SS00001573	NPR1	0.77	natriuretic peptide receptor A/guanylate cyclase A (atrionatriuretic peptide receptor A)
SS00007009	LOC57228	0.77	hypothetical protein from clone 643
SS00006949	EMILIN2	0.75	elastin microfibril interfacer 2
SS00006914	DSIPI	0.72	delta sleep inducing peptide, immunoreactor
SS00005801	HYAL2	0.68	hyaluronoglucosaminidase 2
SS00007835	LOC401137	0.67	hypothetical LOC401137
SS00009553	TEK	0.67	TEK tyrosine kinase, endothelial (venous malformations, multiple cutaneous and mucosal)
SS00009312		0.66	
SS00000205	FAM26B	0.65	family with sequence similarity 26, member B
SS00009154		0.64	
SS00003980	UPK3A	0.63	uroplakin 3A
SS00007236	FGFR3	0.60	fibroblast growth factor receptor 3 (achondroplasia, thanatophoric dwarfism)
SS00004694	PLEK2	0.60	pleckstrin 2
SS00005554	LOC401137	0.60	hypothetical LOC401137
SS00000499	DSTN	0.59	destrin (actin depolymerizing factor)
SS00008566	YWHAH	0.58	tyrosine 3-monooxygenase/tryptophan 5-monooxygenase activation protein, eta polypeptide
SS00000227	CXXC5	0.58	CXXC finger 5
SS00001921	SLC9A3R2	0.57	solute carrier family 9 (sodium/hydrogen exchanger), isoform 3 regulatory factor 2
SS00008590		0.55	
SS00008418	RAI17	0.55	retinoic acid induced 17
SS00006985	DOK4	0.53	docking protein 4
SS00007163	TMEPAI	0.53	transmembrane, prostate androgen induced RNA
SS00003206	ZFP106	0.52	zinc finger protein 106 homolog (mouse)
SS00010071	FAM26B	0.52	family with sequence similarity 26, member B
SS00009566	CLOCK	0.52	clock homolog (mouse)
SS00010488	C10ORF45	0.52	chromosome 10 open reading frame 45
SS00005569	PSAT1	0.51	phosphoserine aminotransferase 1
SS00000439		0.50	
SS00008883	SHCBP1	0.47	likely ortholog of mouse Shc SH2-domain binding protein 1
SS00002193	PSPH	0.46	phosphoserine phosphatase
SS00008822	ETS2	0.45	v-ets erythroblastosis virus E26 oncogene homolog 2

			(avian)
SS00000711	PLK1	0.44	polo-like kinase 1 (Drosophila)
SS00003556	COBLL1	0.43	COBL-like 1
SS00002036	AK1	0.43	adenylate kinase 1
SS00009158	LOC401137	0.42	hypothetical LOC401137
SS00007829	RAMP2	0.42	receptor (calcitonin) activity modifying protein 2
SS00000616	TOP2A	0.34	topoisomerase (DNA) II alpha 170kDa
SS00000501	DCN	-0.57	decorin
SS00001142	KIT	-0.67	v-kit Hardy-Zuckerman 4 feline sarcoma viral oncogene homolog
SS00002946	AREG	-0.85	amphiregulin (schwannoma-derived growth factor)
SS00005446	CXCR4	-0.88	chemokine (C-X-C motif) receptor 4
SS00002290	CXCR4	-0.91	chemokine (C-X-C motif) receptor 4
SS00004185	RGS2	-0.93	regulator of G-protein signalling 2, 24kDa

Table S3: The expression of *a-priori* selected genes in response to the elevated shear stress. Red: p<0.05; blue: p<0.1. The expression values after shear step-up were normalized to the pre step-up (preconditioned) controls. The expression of preconditioned cells were normalized to the static cells. Literature discussing the function and shear response of each selected gene is cited in the table. LSS: laminar shear stress, DSS: disturbed shear stress.

	Preconditioned cells (normalized to static cells)	During adaptation (normalized to preconditioned cells) 5	15	45	90	180	360
Inflammatory and adhesion genes							
ICAM1	-0.50	-0.12	0.01	0.10	-0.03	0.01	0.17
	Inflammatory adhesion molecule (12, 14, 17, 20). LSS: ↓ (3).						
VCAM1	-1.98	0.00	0.14	0.07	-0.19	-0.32	-0.31
	Inflammatory adhesion molecule (12, 14, 17, 20). LSS: ↓ (3, 8); DSS: ↑ (3)						
CCL2	1.18	-0.21	0.15	-0.02	0.01	-0.01	0.23
	MCP1, Inflammatory molecule (14, 17, 20). LSS:↓(3, 21) or biphasic(28); DSS: ↑ (3)						
SELE	-0.25	-0.37	-0.16	-0.06	-0.26	-0.18	-0.07
	Adhesion molecule, E-selectin (12, 14, 17, 20). LSS: ↓ (3); DSS: ↑ (3)						
FOS	-0.24	0.21	0.21	0.00	-0.18	0.92	-0.22
	c-fos gene, activating protein-1, inflammatory (2, 23)						
JUN	-1.69	-0.04	0.17	0.27	0.26	0.02	0.08
	c-jun gene, activating protein-1, inflammatory (2, 23). LSS: ↓ (15)						
KLF2	1.81	-0.13	0.31	0.76	1.50	1.51	1.56
	Inflammatory regulation transcription factor (19, 27, 31). LSS: ↑ (8, 27)						
KLF4	1.83	0.14	0.17	0.45	0.92	1.17	1.30
	Inflammatory regulation transcription factor (13). LSS: ↑(13, 32)						
BMP4	-2.17	-0.10	0.00	-0.04	-0.32	-0.23	-0.17
	Activates inflammatory (16, 29). LSS: ↓ (4, 21); DSS: ↑ (3)						
RELA	-0.11	-0.05	0.06	-0.02	0.03	0.07	0.11
	p65, NFκB (14, 17, 20)						
NFKBIA	-1.31	-0.07	0.08	0.01	0.11	0.10	0.13
	NFκB inhibitor, IκBα (14, 17, 20). LSS: ↓(30)						
IL8	0.95	-0.63	-0.54	-0.91	-0.80	-0.85	-0.87
	Inflammatory chemokine (14, 17, 20). LSS: ↑(5, 6)						
Vasomotion							
NOS3	0.37	0.19	0.46	0.52	0.30	0.38	0.94
	eNOS (7, 11). LSS: ↑ (8)						
EDN1	-0.98	0.00	0.01	0.11	0.01	-0.14	0.01
	Endothelin-1 (11). LSS: ↓(10, 21)						
Caveolin-1	-1.39	-0.08	-0.01	0.08	-0.10	-0.25	-0.25
	Caveolin-1 (7, 11). LSS: ↓(4, 8, 21, 35)						
Oxidative state regulators							
SOD2	0.33	-0.36	-0.24	-0.51	-0.34	-0.27	-0.49
	cytoprotective, MnSOD (25). LSS: ↑ (8); DSS: ↓ (3)						
GADD45β	-0.68	-0.32	0.22	0.48	0.98	0.61	0.41
	cytoprotective gene (25). LSS: ↑ (18) or slightly ↓ (25)						
HMOX1	0.53	-0.12	0.08	-0.13	0.12	0.45	0.77
	anti-oxidative, cytoprotective and anti-inflammatory gene (22, 33). LSS: ↑ (21)						

1. Lock-In Amplifier Start-Up Kit: National Instrument, 2002.
2. **Ahmad M, Theofanidis P, and Medford RM.** Role of activating protein-1 in the regulation of the vascular cell adhesion molecule-1 gene expression by tumor necrosis factor-alpha. *J Biol Chem* 273: 4616-4621, 1998.
3. **Brooks AR, Lelkes PI, and Rubanyi GM.** Gene expression profiling of human aortic endothelial cells exposed to disturbed flow and steady laminar flow. *Physiological genomics* 9: 27-41, 2002.
4. **Chen BP, Li YS, Zhao Y, Chen KD, Li S, Lao J, Yuan S, Shyy JY, and Chien S.** DNA microarray analysis of gene expression in endothelial cells in response to 24-h shear stress. *Physiol Genomics* 7: 55-63, 2001.
5. **Cheng M, Li Y, Wu J, Nie Y, Li L, Liu X, Charoude HN, and Chen H.** IL-8 induces imbalances between nitric oxide and endothelin-1, and also between plasminogen activator inhibitor-1 and tissue-type plasminogen activator in cultured endothelial cells. *Cytokine* 41: 9-15, 2008.
6. **Cheng M, Liu X, Li Y, Tang R, Zhang W, Wu J, Li L, Liu X, Gang Y, and Chen H.** IL-8 gene induction by low shear stress: pharmacological evaluation of the role of signaling molecules. *Biorheology* 44: 349-360, 2007.
7. **Cunningham KS and Gotlieb AI.** The role of shear stress in the pathogenesis of atherosclerosis. *Lab Invest* 85: 9-23, 2005.
8. **Dekker RJ, van Soest S, Fontijn RD, Salamanca S, de Groot PG, VanBavel E, Pannekoek H, and Horrevoets AJ.** Prolonged fluid shear stress induces a distinct set of endothelial cell genes, most specifically lung Kruppel-like factor (KLF2). *Blood* 100: 1689-1698, 2002.
9. **DeMaio L, Tarbell JM, Scaduto RC, Jr., Gardner TW, and Antonetti DA.** A transmural pressure gradient induces mechanical and biological adaptive responses in endothelial cells. *Am J Physiol Heart Circ Physiol* 286: H731-741, 2004.
10. **Eskin SG, Turner NA, and McIntire LV.** Endothelial cell cytochrome P450 1A1 and 1B1: up-regulation by shear stress. *Endothelium* 11: 1-10, 2004.
11. **Feletou M and Vanhoutte PM.** Endothelial dysfunction: a multifaceted disorder (The Wiggers Award Lecture). *Am J Physiol Heart Circ Physiol* 291: H985-1002, 2006.
12. **Galkina E and Ley K.** Vascular adhesion molecules in atherosclerosis. *Arterioscler Thromb Vasc Biol* 27: 2292-2301, 2007.
13. **Hamik A, Lin Z, Kumar A, Balcells M, Sinha S, Katz J, Feinberg MW, Gerzsten RE, Edelman ER, and Jain MK.** Kruppel-like factor 4 regulates endothelial inflammation. *J Biol Chem* 282: 13769-13779, 2007.
14. **Hansson GK and Libby P.** The immune response in atherosclerosis: a double-edged sword. *Nat Rev Immunol* 6: 508-519, 2006.
15. **Himburg HA, Dowd SE, and Friedman MH.** Frequency-dependent response of the vascular endothelium to pulsatile shear stress. *Am J Physiol Heart Circ Physiol* 293: H645-653, 2007.
16. **Jo H, Song H, and Mowbray A.** Role of NADPH oxidases in disturbed flow- and BMP4- induced inflammation and atherosclerosis. *Antioxid Redox Signal* 8: 1609-1619, 2006.
17. **Libby P.** Inflammation in atherosclerosis. *Nature* 420: 868-874, 2002.
18. **Lin K, Hsu PP, Chen BP, Yuan S, Usami S, Shyy JY, Li YS, and Chien S.** Molecular mechanism of endothelial growth arrest by laminar shear stress. *Proceedings*

of the National Academy of Sciences of the United States of America 97: 9385-9389, 2000.

19. **Lin Z, Kumar A, SenBanerjee S, Staniszewski K, Parmar K, Vaughan DE, Gimbrone MA, Jr., Balasubramanian V, Garcia-Cardena G, and Jain MK.** Kruppel-like factor 2 (KLF2) regulates endothelial thrombotic function. *Circ Res* 96: e48-57, 2005.

20. **Lusis AJ.** Atherosclerosis. *Nature* 407: 233-241, 2000.

21. **McCormick SM, Eskin SG, McIntire LV, Teng CL, Lu CM, Russell CG, and Chittur KK.** DNA microarray reveals changes in gene expression of shear stressed human umbilical vein endothelial cells. *Proc Natl Acad Sci U S A* 98: 8955-8960, 2001.

22. **Morse D and Choi AMK.** Heme oxygenase-1: from bench to bedside. *Am J Respir Crit Care Med* 172: 660-670, 2005.

23. **Nagel T, Resnick N, Dewey CF, Jr., and Gimbrone MA, Jr.** Vascular endothelial cells respond to spatial gradients in fluid shear stress by enhanced activation of transcription factors. *Arterioscler Thromb Vasc Biol* 19: 1825-1834, 1999.

24. **Novak L, Neuzil P, Pipper J, Zhang Y, and Lee S.** An integrated fluorescence detection system for lab-on-a-chip applications. *Lab Chip* 7: 27-29, 2007.

25. **Partridge J, Carlsen H, Enesa K, Chaudhury H, Zakkar M, Luong L, Kinderlerer A, Johns M, Blomhoff R, Mason JC, Haskard DO, and Evans PC.** Laminar shear stress acts as a switch to regulate divergent functions of NF-kappaB in endothelial cells. *FASEB J* 21: 3553-3561, 2007.

26. **Rasooly A and Herold KE.** *Biosensors and biodetection : methods and protocols*. New York: Humana Press, 2009.

27. **SenBanerjee S, Lin Z, Atkins GB, Greif DM, Rao RM, Kumar A, Feinberg MW, Chen Z, Simon DI, Luscinskas FW, Michel TM, Gimbrone MA, Jr., Garcia-Cardena G, and Jain MK.** KLF2 Is a novel transcriptional regulator of endothelial proinflammatory activation. *J Exp Med* 199: 1305-1315, 2004.

28. **Shyy YJ, Hsieh HJ, Usami S, and Chien S.** Fluid shear stress induces a biphasic response of human monocyte chemotactic protein 1 gene expression in vascular endothelium. *Proceedings of the National Academy of Sciences of the United States of America* 91: 4678-4682, 1994.

29. **Sorescu GP, Song H, Tressel SL, Hwang J, Dikalov S, Smith DA, Boyd NL, Platt MO, Lassegue B, Griendling KK, and Jo H.** Bone morphogenic protein 4 produced in endothelial cells by oscillatory shear stress induces monocyte adhesion by stimulating reactive oxygen species production from a nox1-based NADPH oxidase. *Circ Res* 95: 773-779, 2004.

30. **Sun H-W, Li C-J, Chen H-Q, Lin H-L, Lv H-X, Zhang Y, and Zhang M.** Involvement of integrins, MAPK, and NF-kappaB in regulation of the shear stress-induced MMP-9 expression in endothelial cells. *Biochem Biophys Res Commun* 353: 152-158, 2007.

31. **van Thienen JV, Fledderus JO, Dekker RJ, Rohlena J, van Ijzendoorn GA, Kootstra NA, Pannekoek H, and Horrevoets AJ.** Shear stress sustains atheroprotective endothelial KLF2 expression more potently than statins through mRNA stabilization. *Cardiovasc Res* 72: 231-240, 2006.

32. **Villarreal G, Zhang Y, Larman HB, Gracia-Sancho J, Koo A, and Garcia-Cardena G.** Defining the regulation of KLF4 expression and its downstream

transcriptional targets in vascular endothelial cells. *Biochem Biophys Res Commun* 391: 984-989.

33. **Wagener FADTG, Volk H-D, Willis D, Abraham NG, Soares MP, Adema GJ, and Figdor CG.** Different faces of the heme-heme oxygenase system in inflammation. *Pharmacol Rev* 55: 551-571, 2003.

34. **Yang B, Tan F, and Guan Y.** A collinear light-emitting diode-induced fluorescence detector for capillary electrophoresis. *Talanta* 65: 1303-1306, 2005.

35. **Zhao Y, Chen BPC, Miao H, Yuan S, Li Y-S, Hu Y, Rocke DM, and Chien S.** Improved significance test for DNA microarray data: temporal effects of shear stress on endothelial genes. *Physiological genomics* 12: 1-11, 2002.